Desalination and Water Treatment
www.deswater.com

doi:10.5004/dwt.2021.27244

226 (2021) 372–381
June

Definitive screening design (DSD) optimization of methyl orange adsorption onto Moroccan clay

A. Mansouri[a], A. Ait Aghzzaf[b], K. Draoui[a,*]

[a]*Laboratoire des Matériaux et Systèmes Interfaciaux, Faculté des Sciences, Université Abdelmalek Essaadi, Tétouan, Morocco, emails: khdraoui@gmail.com/kdraoui@uae.ac.ma (K. Draoui), amal11.mansouri@gmail.com (A. Mansouri)*
[b]*Laboratoire des Sciences Appliquées et Didactique, Ecole Normale Supérieure, Université Abdelmalek Essaadi, Tétouan, Morocco, email: a.aitaghzzaf@uae.ac.ma*

Received 29 September 2020; Accepted 19 March 2021

ABSTRACT

The dye molecules are scarcely biodegradable. They are stable to light and oxidizing agents, which makes their effluent treatment extremely difficult. In this work, the adsorption of methyl orange dye has been carried out using raw clay samples taken from the Jbel Lehbib region (North of Morocco) in an aqueous medium. The experiments were designed according to the definitive screening design (DSD) method. The DSD of the experiment aimed to evaluate the effect of six factors: initial solution pH, initial concentration of methyl orange dye, clay mass, stirring speed, and the temperature and contact time. Adsorbent material properties were investigated by means of X-ray diffraction and Fourier transform infrared spectroscopy. The adsorption tests were carried out in a batch system, and each experimental parameter was changed within its range. Based on the results obtained, a reduced quadratic model was determined to best fit the experiment data, and the most significant factors were found to be: pH, initial concentration, and quadratic term pH × pH. Detailed analysis of the effect of different factors as well as their interaction on the removal has been carried out as well. Maximum removal of 69% occurred at the following optimum conditions: pH = 3 and initial concentration of the dye 600 mg/L.

Keywords: Clay; Dye adsorption; Response surface; Optimization; Definitive screening design

1. Introduction

Dyes are widely used in various industries such as textile [1,2], leather tanning, pulp mills [3,4], and plastic manufacturing [5]. They can be found in hair dyes [6], technological foods [7,8], as well as electrochemical photocells [9]. Other uses of synthetic dyes include efficiency control of wastewater treatment and purification [10,11]. Dye models can also serve as a tool to obtain the specific surface area and to characterize the surface texture [12].

Dyes are known for their chemical stability and intractability. Thus, they are very dangerous to health due to their high toxicity and cancerogenous risk. If the industrial effluents are discharged without any treatment, dyes can harm the environment, and lead to the destruction of aquatic living organisms and soil degradation [13,14]. To protect the environment from their hazards, extensive research has been carried out to develop a sustainable and economical treatment process that efficiently manages dyeing effluents, and reduces their negative impact on the environment. In this perspective, many physicochemical and biological processes were developed to eliminate dyes from wastewater such as: Fenton oxidation, photochemical degradation, advanced oxidation process, reverse osmosis, membrane separation, coagulation, etc. [15–17].

The adsorption process is considered to be the most simple and economical technique used to remove dyes from wastewater [18,19]. It is relatively easy to use for higher volume liquid discharges treatment. The adsorption process can

* Corresponding author.

be performed using several adsorbents such as biomass (biosorption), resin, dendrimer [20–28].

Activated carbon adsorbents generally have a high adsorption capacity of hazardous compounds [29,30]. Nonetheless, it is very expensive and difficult to regenerate. Therefore, the use of new materials as economical alternatives would make this type of process much more cost-effective. In this perspective, clay materials constitute an efficient alternative to activated carbon [31,32]. This mineral resource is characterized by having a phyllosilicate structure, high specific surface area, as well as significant ion exchange capacity and micrometric particle size (less than 2 μm). These properties are often improved by the swelling properties.

In general, a given target or phenomena in nature can be affected by many parameters. A number of experiments are required to assess the impact of these parameters, and the more parameters there are, the more experiments we need, which can grow out of proportion. Hence, the need for a Design of Experiment system that provides such assessment with a reasonable amount of experiments.

Since the experiments are generally costly and time-consuming. In order to overcome these limitations, several strategies were oriented toward the use of statistical models to highlight the significant factors impacting the target. These techniques are known as the screening design of experiments. Recently, several works have shown that the definitive screening design (DSD) can contribute to the elucidation of the factors that most affect the adsorption at the solid/liquid interface [33–35].

In the present work, the adsorption of Methyl Orange by clays sampled locally from Jbel Lehbib (Morocco) was performed. This natural, readily available, and cost-effective adsorbent, was used without any pre-treatment. Six parameters were considered in testing this adsorbent: pH, adsorbent mass, initial concentration of dye, stirring speed, temperature, and exposure contact time. Methyl Orange serves as a model compound for common water-soluble azo dyes, which are widely used in chemical, textile, and paper industries. These dyes are particularly harmful to the environment.

Due to the high number of values that the factors can take, and thereafter the large number of experiments to do, this study starts with the experimental design method (EDM) in order to screen off the most influential parameters on the adsorption process between clay and Methyl Orange. This approach is based on the fact that a well-organized experiment will produce, in most cases, sound analysis, and a better statistical interpretation of the results. The design of the experiment allows the organization of a multi-parameter experiment in a rational and cost-effective way. It consists of yielding high-quality results, and a maximum data collection while running the minimum number of experiments possible. It also allowed building mathematical models using only the parameters that significantly affect the adsorption process.

The EDM is a homogenous set of tools and algebraic statistical methods, aiming to establish and analyze the relations between the studied variables (responses) and their supposed variation sources (factors). This analysis can be qualitative: screening analysis (determination of influent factors) or quantitative: response surface methodology (RSM) (response variations according to influent factors) [36–40].

2. Materials and techniques

2.1. Materials

The raw clay, labeled JBLH, was sampled from the Jbel Lehbib region located in the north of Morocco (Fig. 1). Before its first use, the sample was finely ground using a specific ceramic mortar. The reason behind this operation is to prevent contamination of these raw clay's chemical composition. The resulting powder was sieved to have a size less than 120 μm. In this study, raw clay was considered without any modification of its chemical composition. The adsorption performance is carried out using the methyl orange dye.

The methyl orange, provided by ma-Aldrich (Chimie S.a.r.l., Lyon, France), is a very toxic dye. Its chemical structure is illustrated in Fig. 2. The general chemical formulation of the methyl orange is $C_{14}H_{14}N_3NaO_3S$ and a molecular weight of 327.34 g/mol.

2.2. Clay characterization

The clay mineral phase was characterized by mean X-ray diffraction (XRD) using the diffractometer Brucker D8 advances with the radiation CuKα (λ = 1.54060 nm). The data were collected at 2θ in the range of 10°–80°. The different functional surface groups were investigated by Fourier transform infrared spectroscopy mode ATR-FTIR (Perkin Elmer spectrum TWO). The clay fine powder IR spectra were scanned in the range of wavelengths 400–4,000 cm^{-1}.

The cation exchange capacity (CEC) of the raw clay was determined by placing 0.5 g of dry clay (JBLH) in 100 mL sodium chloride 0.1 M. Next, the suspension was stirred for 24 h and then filtered. The clay was washed by ethanol 3 times to remove excess salt. The sodium (Na^+) exchanged clay were stirred in ammonium chloride solution 0.1 M for 24 h and then the exchange sodium cation was measured by flame photometry using JENWAY flame photometer [41].

The CEC is expressed in meq/100 g.

The value of CEC is given by the following equation:

$$\mathrm{CEC} = \frac{C_{Na^+} \times V}{m} 100 \quad (1)$$

where C_{Na^+} is the concentration of extracted sodium (mmol/L); V is the solution volume (L); m is the oven-dry sample weight (g).

The CEC of raw clay (JBLH) was found to be 39 meq/100 g. It matches well those of clays with moderate swelling properties.

2.3. Adsorption experiment

The adsorption experiments were conducted in batch mode at different initial values of pH, temperature, initial dye concentration, contact time, agitation speed, and clay mass. The tests were carried out by introducing different amounts of adsorbent into a volume of 25 mL of dye solution, and then the glass tubes were shaken to equilibrium at different speeds. After centrifugation separation, the supernatant concentration was determined using a UV-visible spectrometer at λ = 464 nm (Jasco, Lisses-France) [42–44].

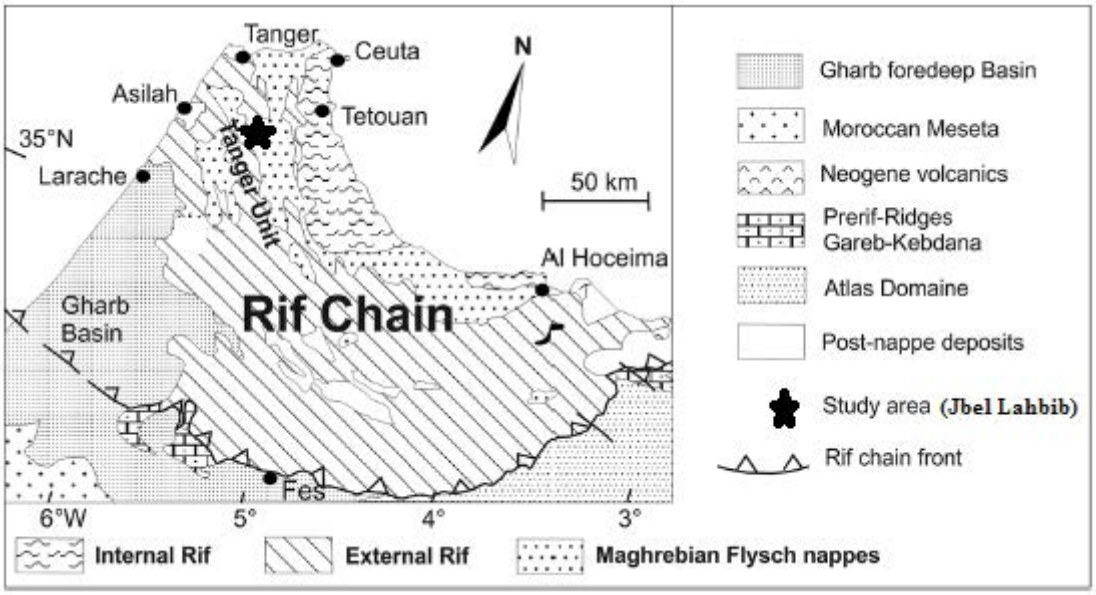

Fig. 1. Geographical location of the sampling area in the Rif chain (Morocco).

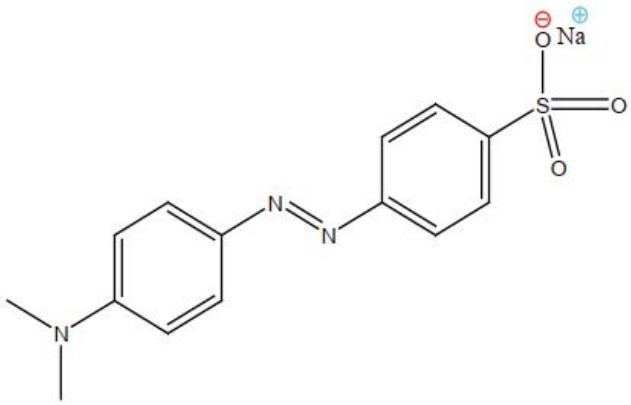

Fig. 2. Methyl Orange (MO) chemical structure.

The removal efficiency (%R) of the orange methyl adsorbed on the clay was calculated according to the following equation:

$$\%R = 100 \times \frac{\left(C_0 - C_e\right)}{C_0} \tag{2}$$

where %R, C_0, and C_e are, respectively, removal efficiency, initial, and equilibrium concentration of MO in the solution (mg/L).

3. Definitive screening experimental design

The DSD, which is an RSM, offers an alternative to the previous experimental design. The DSD was proposed for the first time in 2011 by Jones and Nachtsheim [35] and it is carried out in two stages: the first stage consists of screening the most influencing factors on the response variable, which is the effectiveness of the dye removal in this study. In the second stage, we evaluate the response considering only the factors obtained from the first stage. The main objective of the DSD is to provide the factors that impact significantly the response variable, and then find the optimal condition where the response reaches its optimal or peak value.

Table 1
Variation domain of the experimental factors (coded values)

Factor name	Symbol	Low level	Center	High level
		–1	0	1
Contact time (h)	X_1	2	3	4
C_i (MO) (mg/L)	X_2	50	325	600
Clay mass (g)	X_3	0.02	0.11	0.2
Agitation speed (rpm)	X_4	100	175	250
pH	X_5	2	6.5	11
Temperature (°C)	X_6	30	45	60

In this study, the considered six factors that can affect the adsorption of the methyl orange dye by the raw clay are all quantitative factors. Thus, they can be controlled and can adopt all real numerical values in their specified interval of variation, which makes the DSD very useful. Table 1 presents the factors considered and their variation range considered in this work.

The DSD improves and generalizes its antecedents by taking into account new considerations. Unlike the previous experimental designs that are based on two levels, the definitive plans consider three levels per factor. Also, these designs consider the interactions between the factors, which are not supported by other designs like Plackett–Burman plan [45]. The importance of such interactions is considered by classical statistical models such as generalized quadratic and

nonlinear models. Moreover, the DSD may be used for both screening and optimization of experimental conditions. The DSD can handle both quantitative and categorical factors. Indeed, quantitative factors are run at three levels, which allow the estimation of both linear and quadratic effects of predictors.

It is very clear that these new features make DSD the most suitable tool for modeling and optimization of the experiment process. In addition, the DSD provides more details on the relationship between the factors or predictors and the response variable [33–35,46,47], and this feature increases their accuracy and minimizes the discrepancies between the experimental values of a test and those predicted by the model.

Table 1 shows the factors and the variation range of each explanatory variable considered in this study. The DSD adopted is generated by software Minitab.

4. Results and discussion

4.1. Characterization of raw clay

The XRD pattern of raw clay (JBLH) of Fig. 3 shows peaks characteristic of phyllosilicates at 2θ = 5.71°, 8.95°, and 12.35° corresponding to the basal spacing of 15.48, 9.97, and 7.16 Å, respectively. The reflection at 15.48 Å is considerably more intense than those observed at 9.97 and 7.16 Å. The distance 15.48 Å is typical of the basal distance d_{001} of a smectite clay saturated with a hydrated divalent cation such as Ca^{2+}, its sphere of hydration contains two equivalents of water layers in the usual conditions of humidity [48–50]. While peaks observed at 9.97 Å correspond to illite [51] and those at 12.35° (7.16 Å) and 25° (3.5 Å) reveals the presence of kaolinite (JCPDS file: 00-029-1488).

The reflections observed at 2θ = 20.99° (4.23 Å) and 26.70° (3.34 Å) correspond to the quartz (JCPDS file: 99-101-2545), whereas those present at 36.28° (d = 2.47 Å) are attributed to carbonate (JCPDS file: 01-089-1304).

4.2. Fourier transform infrared

FTIR spectroscopy was used for the surface groups characterizing the raw clay sample. The spectra (Fig. 4) showed three principal absorption bands between 3,200–3,800, 1,600–1,700, and 450–1,200 cm^{-1}. The band observed at 3,694 cm^{-1} corresponds to the elongation vibrations of the (OH) groups [52–54]. The band located at 3,624 cm^{-1} corresponds to the elongation vibrations of the internal OH groups in Al_2OH [50,51,55]. The band at 1,642 cm^{-1} is attributed to the binding vibrations of adsorbed water [54]. The intense band between 900 and 1,200 cm^{-1} and centered at 989 cm^{-1} corresponds to the valence vibrations of Si–O group of kaolinite or quartz [56,57]. The corresponding deformation vibration bands are observed at 517 and 469 cm^{-1} [55]. The bands between 795 and 748 cm^{-1} results from Si–O–Al linkage, and gives rise also to a band around 789 cm^{-1} [43]. The absorption bands around 797 and 779 cm^{-1} correspond to quartz [58]. The bands at 3,624 and 912 cm^{-1} are characteristic of dioctahedral smectites and originate from stretching (υ) and deformation (δ) vibrations, respectively, of hydroxyls in the [AlAl–OH] configuration [59]. Furthermore, the well-defined band observed at 3,694 and 689 cm^{-1} correspond to kaolinite [55]. A week band around 1,434 cm^{-1} confirms the presence of a small amount of carbonate.

These results are in agreement with those given by XRD characterization. They confirm that the raw clay (JBLH) is composed of smectite, illite, kaolinite, quartz, and calcite.

4.3. DSD optimization

The DSD generalizes the linear one by adding the quadratic and interaction effects between factors. In the DSD, the response variable Y is expressed by a second-order polynomial of the explanatory variables X [33,34,46,47]. The general form of this model is given by the following equation:

$$Y = \alpha_0 + \sum_{i=1}^{n} \alpha_i X_i + \sum_{i=1}^{n} \alpha_{ii} X_{ii}^2 + \sum_{i,j=1(i\neq j)}^{n} \alpha_{ij} X_i X_j \quad (3)$$

where Y represents the response variable; α_0 is the medium values of the response; α_i is the coefficient of the linear term X_i; α_{ii} are the coefficient of the quadratic term X_{ii}^2; α_{ij} is the coefficient of the interaction between terms X_i and X_j.

Table 2 presents the data and the results related to this experiment. Sixteen tests have been conducted, the first 13 indexed from 1 to 13 in column test are used to fit the model parameters, and the other three are used as validation data. The column named test gives the index of the

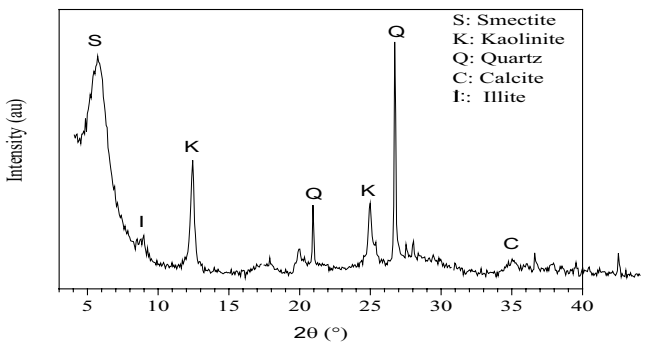

Fig. 3. XRD patterns of the Jbel Lahbib (JBLH) raw clay powder.

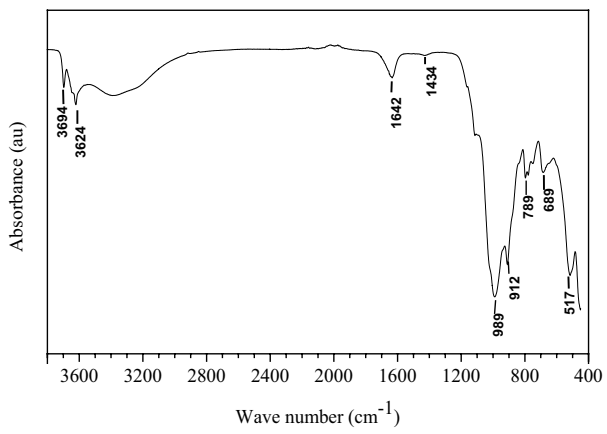

Fig. 4. FTIR spectra of Jbel Lahbib raw clay.

Table 2
Definitive screening plan matrix test for MO adsorption on Jbel Lahbib raw clay

	Test	Agitation speed (rpm)	Time (h)	pH	C_i (MO) (mg/L)	m (g)	T (°C)	%R Obs	%R Pred
Experimental	1	175	2	2	50	0.02	30	79.95	76.2
tests	2	100	4	6.5	600	0.02	30	11.15	13.97
	3	250	4	11	50	0.11	30	–8.33	–6.82
	4	100	2	11	325	0.2	30	7.97	1.51
	5	250	3	2	600	0.2	30	95.05	92.86
	6	250	2	11	600	0.02	45	8.07	9.84
	7	175	3	6.5	325	0.11	45	10.87	5.64
	8	100	4	2	50	0.2	45	79.73	76.2
	9	100	3	11	50	0.02	60	–12.74	–6.82
	10	250	4	2	325	0.02	60	77.86	76.2
	11	100	2	2	600	0.11	60	90.03	92.86
	12	250	2	6.5	50	0.2	60	–5.11	–2.69
	13	175	4	11	600	0.2	60	12.52	9.84
Validation	1	100	4	11	600	0.02	60	13.97	9.84
tests	2	250	2	2	600	0.2	60	87.66	92.86
	3	250	4	2	600	0.02	30	94.75	92.86

test experiment, column agitation speed gives the stirring speed, column time gives the values of contact time, the values of pH considered are given in the column pH, column C gives the initial concentration values of methyl orange dye, the column m presents the values of the clay mass used, and column T gives the temperature values considered. Finally, %R obs and %R Pred give, respectively, the removal percentage obtained by the tests achieved and those predicted by the model.

Determination of the effects of main factors on methyl orange (MO) adsorption was performed using a MiniTab software considering the stepwise selection of factors and considering level $\alpha = 0.05$. Eq. (2) shows that factors: pH, initial concentration, and the quadratic term pH × pH are the most significant factors on the response variable, with a negative value of the pH coefficient, and positive value for the initial concentration of the dye and the quadratic terms pH × pH. This means that an increase in pH leads to a reduction in the percentage of removal and that an increase in the initial concentration leads to an increase in the adsorption efficiency of the clay. In addition, the obtained mode shows that the quadratic factor pH × pH is very important because of the high value of its coefficient in the general model equation. The mathematical model that explains the relationship between the factors and the response variable is given by Eq. (4), considering the coded values of the factors. Eq. (4) will be used later to validate our model by considering new experiences not considered in the learning phase:

$$\%R = 5.64 - 41.51\text{pH} + 8.33C_i + 37.38\,\text{pH} \times \text{pH} \quad (4)$$

4.3.1. Adequation straight line

The graph in Fig. 5 clearly shows the great similarity between the experimental data and the one obtained by the model. The scatter plot of the theoretical yield versus the experimental yield is very close to the resulting regression line, which shows the strong linear dependence between the theoretical and the experimental yield values. This verdict justifies the quality of the obtained model.

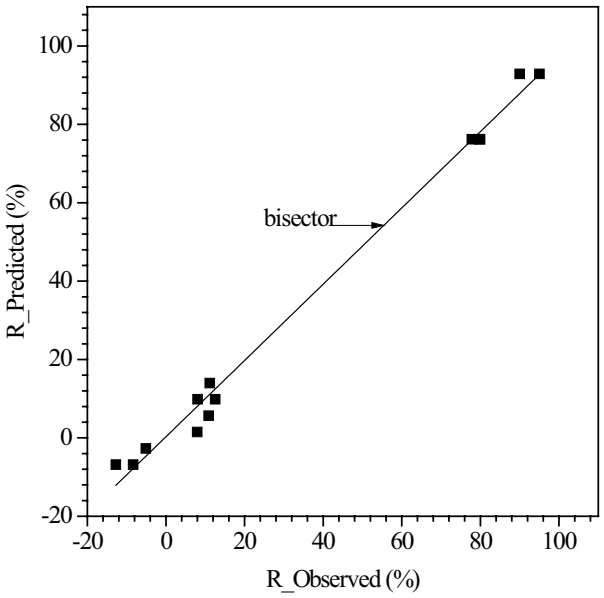

Fig. 5. Theoretical removal in terms of experimental data.

4.3.2. Model validation

To validate and confirm the previously obtained results that showed the quality of the proposed model, three new experiences, that were not part of the learning process, were

considered. The results obtained from these three experiments further confirmed the learning outcomes. From the graph in Fig. 6, where the first 13 values represent the training data and the last three represent those of validation, the results show that the model maintains the same behavior between training and validation data. In addition, the model presents nearly the same squared error over the training and validation data, which means that the fitted model has a good generalization quality.

4.3.3. Analysis of variance

Table 3
Analysis of variance (ANOVA) considering the coded data

Term	Coeff	CoefErT	*T*-value	*P*-value	VIF
Constant	5.64	2.82	2.00	0.077	
pH	–41.51	1.54	–26.89	0.000	1.00
C_i (MO)	8.33	1.54	5.40	0.000	1.00
pH × pH	37.38	3.21	11.63	0.000	1.00

Where:

- Coeff is the estimated value of the model parameters,
- CoefErt is the estimated standard deviation of the error in measuring the Coeff,
- *T*-value measures the relationship between the coefficient value (Coeff) and its standard error (CoefErT) (*T*-value = Coeff/CoefErT)
- *P*-value is the probability that measures the degree of certainty with which it is possible to invalidate the value of Coeff.
- Finally, VIF is the variance inflation factor and indicates the extent to which the variance of a coefficient is increased by the correlations between the predictors of the model.

The results of the Analysis of variance is shown in Table 3. In relation to the coefficient of the pH factor, one notices that it is of negative sign, therefore, pH negatively impacts the response variable. An increase in the pH value causes a decrease in the percentage of adsorption removal of the studied clay. Consequently, the clay adsorbs well in an acidic medium. Another observation is that the absolute value of the coefficient of pH in the model obtained is much higher than those of the other factors, which implies its importance for the clay adsorption capacity. In addition, its *P*-value is less than 0.05 significance threshold, altogether clearly stating that the value of the pH coefficient is very significant. The same analysis can be done for the initial concentration and the quadratic term pH × pH. The VIF values that are very close to 1 indicate the absence of multicollinearity that can undermine the statistical significance of independent factors on the response variable.

4.3.4. Analysis of the Pareto diagram

The purpose of the Pareto diagram is to illustrate the factors that have a significant statistical impact on the response variable; also this graphic shows the level of impact of each factor on the response variable. In the Pareto diagram, the bars that intersect the line of reference, line with the value 2.26 in our case (Fig. 7), represent the significant factors with a precision level $1 - \alpha$. In this study, the value of α is fixed at 0.05, which guarantees with 95% accuracy that the level factor obtained is around the given value. The Pareto diagram analyzes the standardized effects of various factors on the response variable, taking into account the quadratic effect of each factor as well as the interactions between two factors.

Fig. 7 presents the Pareto diagram of the normalized effects of the factors considered in the definitive screening plan adopted in this study. The significance threshold line for alpha = 0.05 is 2.26. At this level of significance, the most important factor is the *C* which is the pH, followed by the

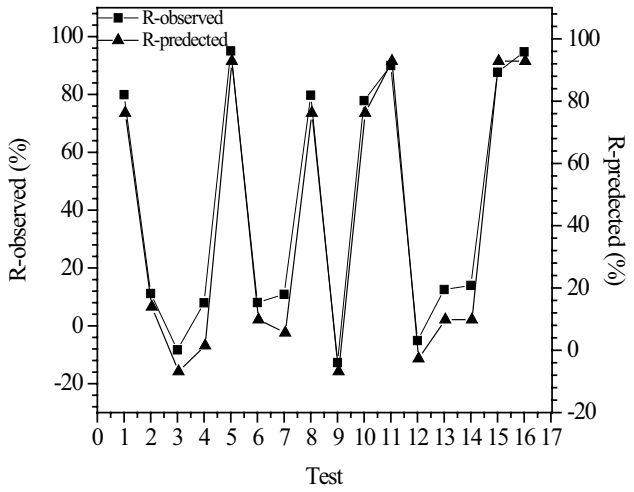

Fig. 6. Comparison of experimental and predicted removal efficiency.

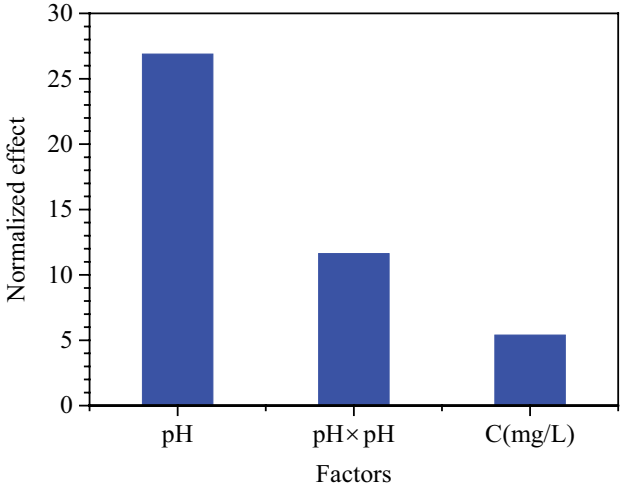

Fig. 7. Pareto diagram of the normalized effects in MO adsorption on Jbel Lahbib raw clay (answer = %*R* removal, α = 0.05).

quadratic term CC, quadratic factors pH × pH, and the term *D* which is the initial concentration of the considered clay. The rest of factors that are not shown in the Pareto chart are statistically not significant. This means that the response variable can be expressed only by three factors *C*, CC, and *D* with an acceptable level of accuracy.

From the Pareto diagram, it is clear that the factors pH and initial concentration of the dye are very significant compared to the other ones. The quadratic term CC is statistically significant and its impact on the response variable is very notable. The other factors do not seem to have a significant impact on the response variable.

4.3.5. Coefficients of determination

Determination coefficients were considered to evaluate the adequacy of the proposed model. In general, three determination coefficients R^2, the adjusted R^2_{aj} and the expected R^2_e are computed. The value of R^2 characterizes the proportion of the response variation given by the proposed model. A high R^2 value, in general, indicates that the model is exhaustive, whereas a weak R^2 indicates that the model proposed does not specify correctly the relationship existing between the factors and the response variable. However, in some cases a high value of R^2 can be misleading because a model with too many factors can fall under the overfitting problem, therefore the model will lose its ability to generalization.

To measure the overfitting that the mathematical model can present the adjusted R^2_{aj} indicator is calculated. R^2_{aj} takes into account the number of factors considered in a model. Another indicator can be computed to verify that the model has a good generalization capacity, it is the expected coefficient of determination R^2_e. Hereafter, if the three indicators, R^2, R^2_{aj}, and R^2_e have high values, close to 100%, this means that the proposed model is of good quality, and can model the relationship between the predictors and the answer correctly. In Table 4, we present the values of the three indicators previously obtained in our work. It is clear that the three coefficients of determination are close to 99%, which justifies once again that the used model is of good quality and has very good generalization ability.

4.4. Optimization process analysis

The model obtained is a nonlinear model, which involves the quadratic terms pH × pH. In the optimization process, the only constraints that have been considered are the margins of variation of each factor. For example, the pH value varies between 2 and 11. More information on the margin variation of each factor is given in Table 1. The DSD is carried out using Minitab 18 that has a very appropriate and flexible optimization tool, it allows the user to take the optimization process under control by modifying the constraints manually. In addition, the Mintab optimizer has a graphical tool that permits to view of the response variable variation by changing the value of a single factor at a time.

Table 4
Correlation coefficients of the quadratic model

Coefficient	R^2	R^2_{aj}	R^2_e
Values	99.00%	98.66%	98.05%

The graph in Fig. 8 gives a general overview of the output of the optimization provided by Minitab. We can note that the best value of the response variable is obtained at the point (pH = 2, concentration of dye = 600 mg/L), but it is well known that pH = 2 conditions may cause low leaching of the clay, that is why the value of pH was fixed at 3 in order to avoid the degradation of pH factor. From Fig. 8, the optimal operating points (pH = 3 and initial concentration of dye = 600 mg/L) giving maximum MO removal (68.87%), and it is clear that the presence of a curvature at the pH factor means that the effect of the quadratic term pHxpH is statistically significant. This confirms once again the obtained results when studying the effects of the factors treated before.

It is necessary to analyze the contour curves of the obtained function by the mathematical model result in order to deeply understand the behavior of the response variable around the optimum point. The outlines classify the areas of variation of the response variable according to two factors. The following section presents contour curves for our case study.

4.4.1. Contour lines

According to the profiles in Fig. 9, we observe that if we seek a removal rate greater than 80%, it is necessary to consider the pH value equal to 3. Also. It is clear that, the effect of the second factor (initial concentration of the dye in mg/L) has a remarkable influence only when the medium becomes basic, which explains the importance of the pH factor on the response variable.

4.4.2. Response surface

The graph in Fig. 10 shows the response surface of the removal OM dye (%*R*) vs. the significant factors pH and the initial concentration of OM (C_i) only. This graph shows that the response increases as the pH decreases from 11 to 2, whereas the initial concentration does not have a noticeable effect if the pH level is fixed. In this last case, the response variable remains unchangeable. Moreover, it is easy to depict that with a pH equal to 3 the value of the yield remains above 80% regardless of the value of the initial concentration.

Fig. 8. Optimal values for the significant parameters influencing the removal dye (%*R*), and the predicted value together with the lower and upper limits.

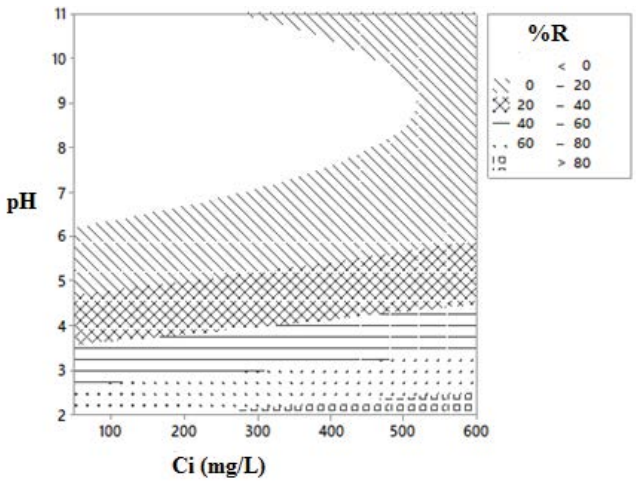

Fig. 9. Optimal values of the significant factors influencing the %*R*.

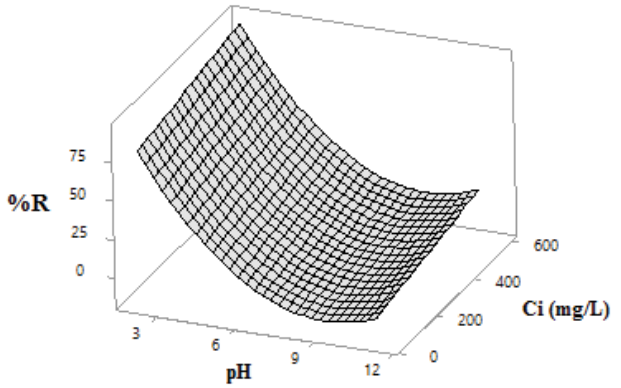

Fig. 10. Response surface plot of the retention (%*R*) vs. pH and initial concentration (C_i) of MO.

5. Conclusion

The present work was devoted to optimizing the adsorption of the orange methyl (OM) by raw clay extracted from the Jbel Lehbib region located in the north of Morocco. The raw clay consisted of phyllosilicates (smectite, illite, and kaolinite) along with quartz and carbonate. This study shows that the used natural clay, whose CEC is around 39 meq/100 g, can efficiently remove the MO dye from aqueous solutions under some optimal experimental conditions. Many factors that affect the adsorption of dye by clay, including pH, initial concentration of the dye (C_i), temperature, the contact time, the clay mass, and the stirring speed are studied and analyzed. Since finding the optimal conditions is not straightforward given the numerous variables; the DSD is successfully used to select the most important factors that impact the adsorption process. The DSD methodology is composed of two major steps. During the first step (screening step), the statistical analysis and Pareto graphic singled out two major factors (pH and C_i). The obtained mathematical model of the removal dye response (%*R*) has three principal terms (pH, C_i, and pH²). Further, the validation tests support the theoretical model giving similar results. During the second step (optimization step), the contour line and response surface confirm that the removal of dye by clay is high in the acidic medium as well as when the initial concentration of dye C_i increases. The maximum removal of 69% was achieved at pH = 3 and initial OM concentration C_i equal to 600 mg/L.

Acknowledgments

This work was financially supported by the CNRST-Morocco, PPR2 Project "Nouveaux Nanocomposites à Base d'Argiles Marocaines et Biopolymères pour la Purification de l'Acide Phosphorique et pour l'Aménagement des Décharges Publiques".

References

[1] B.J. Brüschweiler, S. Küng, D. Bürgi, L. Muralt, E. Nyfeler, Identification of non-regulated aromatic amines of toxicological concern which can be cleaved from azo dyes used in clothing textiles, Regul. Toxicol. Pharm., 69 (2014) 263–272.
[2] L. Jian, M. Chika, R. Laursen, Z. Feng, Z. Yang, L. Wenying, Characterization of dyes in ancient textiles from Yingpan, Xinjiang, J. Archaeol. Sci., 40 (2013) 4444–4449.
[3] C. Montagner, M. Bacci, S. Bracci, R. Freeman, M. Picollo, Library of UV-vis-NIR reflectance spectra of modern organic dyes from historic pattern-card coloured papers, Spectrochim. Acta, Part A, 79 (2011) 1669–1680.
[4] V. Gómez, R. Cuadros, I. Ruisánchez, M.P. Callao, Matrix effect in second-order data: determination of dyes in a tanning process using vegetable tanning agents, Anal. Chim. Acta, 600 (2007) 233–239.
[5] A. Abel, The History of Dyes and Pigments: From Natural Dyes to High Performance Pigments, J. Best, Ed., Colour Design: Theories and Applications, Woodhead Publishing, Cambridge, 2012, pp. 433–470.
[6] C. Brunet, I. Clonier, A. De la Sayette, Nowdays applications of vegetable dyes, La Phytothérapie européenne, 65 (2011) 15–21.
[7] S. Komissarchik, G. Nyanikova, Test systems and a method for express detection of synthetic food, LWT Food Sci. Technol., 58 (2014) 315–320.
[8] P. Giridhar, V. Akshatha, R. Parimalan, A review on annatto dye extraction, Int J. Sci. Rep., 3 (2014) 327–348.
[9] D. Wrobel, A. Boguta, R. Ion, Mixtures of synthetic organic dyes in a photoelectrochemical cell, J. Photochem. Photobiol., A, 138 (2001) 7–22.
[10] N. Bensalaha, M.A. Quiroz Alfaro, C.A. Martínez-Huitle, Electrochemical treatment of synthetic wastewaters containing Alphazurine A dye, Chem. Eng. J., 149 (2009) 348–352.
[11] R.B. Chavan, Chapter 16 – Environmentally Friendly Dyes, M. Clark, Ed., Handbook of Textile and Industrial Dyeing, Vol. 1, Woodhead Publishing Series in Textiles, Woodhead Publishing, Cambridge, 2011, pp. 515–561.
[12] Y. Nilgün, B. Cengiz, Ö. Müşerref, S. Yüksel, Simultaneous determination of cation exchange capacity and surface area of acid activated bentonite powders by methylene blue sorption, Appl. Surf. Sci., 258 (2012) 2534–2539.
[13] Z. Maiyong, M. Dehai, W. Chengjia, D. Jian, D. Guowang, Degradation of methylene blue with H_2O_2 over a cupric oxide nanosheet catalyst, Chin. J. Catal., 34 (2013) 2125–2129.
[14] M. Alok, V.K. Gupta, M. Arti, M. Jyoti, Process development for the batch and bulk removal and recovery of a hazardous, water-soluble azo dye (Metanil Yellow) by adsorption over waste materials (Bottom Ash and De-Oiled Soya), J. Hazard. Mater., 151 (2008) 821–832.
[15] T.H. Bokhari, N. Ahmad, M.I. Jilani, M. Saeed, M. Usman, A. Ul Haq, R. Rehman, M. Iqbal, A. Nazir, T. Javed, UV/H_2O_2, UV/H_2O_2/SnO_2 and Fe/H_2O_2 based advanced oxidation processes

for the degradation of disperse violet 63 in aqueous medium, Mater. Res. Express, 7 (2020) 015531, doi: 10.1088/2053-1591/ab6c15.
[16] I. Bibi, S. Hussain, F. Majid, S. Kamal, S. Ata, M. Sultan, M.I. Din, M. Iqbal, A. Nazir, Structural, dielectric and magnetic studies of perovskite [$Gd_{1-x}M_xCrO_3$ (M = La, Co, Bi)] nanoparticles: photocatalytic degradation of dyes, Z. Phys. Chem., 233 (2019) 1431–1445.
[17] N. Ul-Haq Khan, H.N. Bhatti, M. Iqbal, A. Nazir, Decolorization of Basic Turquise Blue X-GB and Basic Blue X-GRRL by the Fenton's process and its kinetics, Z. Phys. Chem., 233 (2019) 361–373.
[18] T.Y. Mustafa, K.S. Tushar, A. Sharmeen, H.M. Ang, Dye and its removal from aqueous solution by adsorption: a review, Adv. Colloid Interface Sci., 209 (2014) 172–184.
[19] Y. Miyah, M. Idrissi, A. Lahrichi, F. Zerrouq, Removal of a cationic dye – Méthylène Bleu – from aqueous solution by adsorption onto oil shale ash of Timahdit (Morocco), Int. J. Innovative Res. Sci. Eng. Technol., 3 (2014) 15600–15613.
[20] R.K. Mohapatra, P.K. Parhi, S. Pandey, B.K. Bindhani, H. Thatoi, C.R. Panda, Active and passive biosorption of Pb(II) using live and dead biomass of marine bacterium *Bacillus xiamenensis* PbRPSD202: kinetics and isotherm studies, J. Environ. Manage., 247 (2019) 121–134.
[21] S. Sinha, S.S. Behera., S. Das. A. Basu, R.K. Mohapatra, B.M. Murmu, N.K. Dhal, S.K. Tripathy, P.K. Parhi, Removal of Congo Red dye from aqueous solution using amberlite IRA-400 in batch and fixed bed reactors, Chem. Eng. Commun., 205 (2018) 432–444.
[22] B.M. Murmu, S.S. Behera, S. Das., R.K. Mohapatra, B.K. Bindhani, P.K Parhi, Extensive investigation on the study for the adsorption of Bromocresol Green (BCG) dye using activated Phragmites karka, Indian J. Chem. Technol., 25 (2018) 409–420.
[23] S.S. Behera, D. Sourav, P.K. Parhi, S.K. Tripathy, R.K. Mohapatra, M. Debata, Kinetics, thermodynamics and isotherm studies on adsorption of methyl orange from aqueous solution using ion exchange resin Amberlite IRA-400, Desal. Water Treat., 60 (2017) 249–251.
[24] S.S. Behera, S. Das, B.M. Murmu, R.M. Mohapatra, T.R. Sahoo, P.K. Parhi, Kinetics, thermodynamics and isotherm studies on adsorption of methyl violet from aqueous solution using activated bio-adsorbent: Phragmites Karka, Curr. Environ. Eng., 3 (2016) 229–241.
[25] K.H. Park, P.K. Parhi, N.H. Kang, Mineral resource, studies on removal of low content copper from the sea nodule leach liquor using the cationic resin TP 207, Sep. Sci. Technol., 47 (2012) 1531–1540.
[26] H.N. Bhatti, Y. Safa, S.M. Yakout, O.H. Shair, M. Iqbal, A. Nazir, Efficient removal of dyes using carboxymethyl cellulose/alginate/polyvinyl alcohol/rice husk composite: adsorption/desorption, kinetics and recycling studies, Int. J. Biol. Macromol., 150 (2020) 861–870.
[27] I. Sohail, I.A. Bhatti, A. Ashar, F.M. Sarim, M. Mohsin, R. Naveed, M. Yasir, M. Iqbal, A. Nazir, Polyamidoamine (PAMAM) dendrimers synthesis, characterization and adsorptive removal of nickel ions from aqueous solution, J. Mater. Res. Technol., 9 (2020) 498–506.
[28] M. Ahmad, G. Abbas, R. Haider, F. Jalal, G.A. Shar, G.A. Soomro, N. Qureshi, M. Iqbal, A. Nazir, Kinetics and equilibrium studies of eriobotrya japonica: a novel adsorbent preparation for dyes sequestration, Z. Phys. Chem., 233 (2019) 1469–1484.
[29] L. Fei-fei, F. Jin-lin, W. Shu-guang, M. Guang-hui, Adsorption of natural organic matter analogues by multi-walled carbon nanotubes: comparison with powdered activated carbon, Chem. Eng. J., 219 (2013) 450–458.
[30] M. Kumar, R. Tamilarasan, Removal of Victoria Blue using *Prosopis juliflora* bark carbon: kinetics and thermodynamic modeling studies, J. Mater. Environ. Sci., 5 (2014) 510–519.
[31] M. Ahrouch, J.M. Gatica, K. Draoui, D. Bellido, H. Vidal, Honeycomb filters as an alternative to powders in the use of clays to remove cadmium from water, Chemosphere, 259 (2020) 127526, doi: 10.1016/j.chemosphere.2020.127526.
[32] Y. Bentahar, K. Draoui, C. Hurel, O. Ajouyed, S. Khairoun, N. Marmier, Physico-chemical characterization and valorization of swelling and non-swelling Moroccan clays in basic dye removal from aqueous solutions, J. Afr. Earth Sci., 154 (2019) 80–88.
[33] V. Kecić, Đ. Kerkez, M. Prica, O. Lužanin, M. Bečelić-Tomin, D.T. Pilipović, B. Dalmacija, Optimization of azo printing dye removal with oak leaves-nZVI/H_2O_2 system using statistically designed experiment, J. Cleaner Prod., 202 (2018) 65–80.
[34] C. Zhang, W. Chen, J. Xian, D. Fub, Application of a novel definitive screening design to *in situ* chemical oxidation of acid orange-II dye by a Co^{2+}/PMS system, RSC Adv., 8 (2018) 3934–3940.
[35] J. Bradley, J.C. Nachtsheim, A class of three-level designs for definitive screening in the presence of second-order effects, J. Qual. Technol., 43 (2011) 1–15.
[36] R.A. Khera, M. Iqbal, A. Ahmad, S.M. Hassan, A. Nazir, A. Kausar, H.S. Kusuma, J. Niasr, N. Masood, U. Younas, R. Nawaz, M.I. Khan, Kinetics and equilibrium studies of copper, zinc, and nickel ions adsorptive removal on to *Archontophoenix alexandrae*: conditions optimization by RSM, Desal. Water Treat., 201 (2020) 289–300.
[37] M. Salman, M. Shahid, T. Sahar, S. Naheed, M. Ur-Rahman, M. Iqbal, A. Nazir, Development of regression model for bacteriocin production from local isolate of *Lactobacillus acidophilus* MS1 using Box–Behnken design, Biocatal. Agric. Biotechnol., 24 (2020) 101542, doi: 10.1016/j.bcab.2020.101542.
[38] S. Jabeen, S. Ali, M. Nadeem, K. Arif, N. Qureshi, G.A. Shar, G.A. Soomro, M. Iqbal, A. Nazir, U.H. Siddiqua, Statistical modeling for the extraction of eye from natural source and industrial applications, Pol. J. Environ. Stud., 28 (2019) 2145–2150.
[39] P.K. Parhi, K. Sarangi, S. Mohanty, Process optimization and extraction of nickel by hollow fiber membrane using response surface methodology, Miner. Metall. Process., 29 (2012) 225–230.
[40] P.K. Parhi, S. Mohanty, K. Sarangi, Experimental studies and parameter optimization of separation of copper using hollow fiber- supported liquid membrane, Chem. Eng. Commun., 200 (2013) 1237–1250.
[41] Y. Moujahid, R. Bouabid, Mineralogy and charge of Moroccan vertisoil smectite, J. Mater. Environ. Sci., 6 (2015) 3328–3337.
[42] N. Fayoud, S. Alami Younssi, S. Tahiri, A. Albizane, Kinetic and thermodynamicstudy of the adsorption of methylene blue on woodashes, J. Mater. Environ. Sci., 6 (2015) 13295–3306.
[43] J. Baliti, A. Asnaoui, S. Abouarnadasse, l'élimination du bleu de méthylène par une argile naturelle de Taza en milieu aqueux, Int. J. Innovative Res. Adv. Eng., 1 (2014) 2349–2163.
[44] Y. Miyah, M. Idrissi, F. Zerrouq, Study and modeling of the kinetics methylene blue adsorption on the clay adsorbents (pyrophillite, Calcite), J. Mater. Environ. Sci., 6 (2015) 699–712.
[45] J. Goupy, What kind of experimental design for finding and checking robustness of analytical methods?, Anal. Chim. Acta, 544 (2005) 184–190.
[46] J. Antony, Fundamentals of Design of Experiments, J. Antony, Ed., Design of Experiments for Engineers and Scientists, 1st ed., Elsevier, Amsterdam, 2003, pp. 6–16.
[47] M. El-Azazy, A.S. El-Shafie, A. Ashraf, A.A. Issa, Eco-structured biosorptive removal of basic fuchsin using pistachio nutshells: a definitive screening design based approach, J. Appl. Sci., 9 (2019) 4855, doi: 10.3390/app9224855.
[48] G. Brown, G.W. Brindley, X-ray Procedures for clay Minerals Identification, G.W. Brindley, G. Brown, Eds., Crystal Structure of Clay Minerals and Their X-ray Identification, Monograph 5, Mineralogical Society, London, 1980, pp. 305–360.
[49] T. Holtzapffel, Les Minéraux Argileux: Préparation, Analyse Diffractométrique et Détermination, Société Géologique du Nord, Lille, France, 1985.
[50] H.W. Van der Marel, H. Beutelspacher, Atlas of Infrared Spectroscopy of Clay Minerals and Their Admixtures, Elsevier Publishing Company, UK, 1976.
[51] A. Qlihaa, S. Dhimni, F. Melrhaka, N. Hajjaji, A. Srhiri, Physico-chemical characterization of a Moroccan clay, J. Mater. Environ. Sci., 7 (2016) 1741–1750.

[52] L. Bouna, B. Rhouta, F. Daoudi, M. Maury, F. Amjoud, F. Senocq, M.C. Lafont, A. Jada, A. Ait. Aghzzaf, Mineralogical and physico-chemical characterizations of ferruginous beidellite-rich clay from Agadir basin (Morocco), Clays Clay Miner., 60 (2012) 278–290.
[53] N. Nisar, O. Ali, A. Islam, A. Ahmad, M. Yameen, A. Ghaffar, M. Iqbal, A. Nazir, N. Masood, A novel approach for modification of biosorbent by silane functionalization and its industrial application for single and multi-component solute system, Z. Phys. Chem., 233 (2019) 1603–1623.
[54] M. Ritz, L. Vaculíková, E. Plevová, Identification of clay Minerals by infrared spectroscopy and discriminant analysis, Appl. Spectrosc., 64 (2010) 1379–1387.
[55] J.E. Boulingui, C. Nkoumbou, D. Njoya, F. Thomas, J. Yvon, Characterization of clays from Mezafe and Mengono (Ne-Libreville, Gabon) for potential uses in fired products, Appl. Clay Sci., 115 (2015) 132–144.
[56] U.O. Aroke, U.A. El-Nafaty, XRF, XRD and FTIR properties and characterization of HDTMA-Br surface modified organo-kaolinite Clay, Int. J. Adv, 4 (2014) 817–825.
[57] A. Kausar, K. Naeem, T. Hussain, Z. Nazli, H.N. Bhatti, F. Jubeen, A. Nazir, M. Iqbal, Preparation and characterization of chitosan/clay composite for direct Rose FRN dye removal from aqueous media: comparison of linear and non-linear regression methods, J. Mater. Res. Technol., 8 (2019) 1161–1174.
[58] J.S. Bhaskar, P. Gopalakrishnarao, Fourier transform infrared spectroscopic characterization of kaolinite from assam and meghalaya, Northeastern India, J. Mod. Phys., 1 (2010) 206–210.
[59] M. Gourouza, A. Zanguina, I. Natatou, A. Bois, Caractérisation d'une argile mixte du Niger, Rev. CAMES Sci. Struct. Mater., 1 (2013) 29–39.